Oxygen Diffusion through the Disordered Oxide Network during Silicon Oxidation

Angelo Bongiorno and Alfredo Pasquarello

Institut de Théorie des Phénomènes Physiques (ITP), Ecole Polytechnique Fédérale de Lausanne (EPFL), CH-1015 Lausanne, Switzerland

Institut Romand de Recherche Numérique en Physique des Matériaux (IRRMA), CH-1015 Lausanne, Switzerland

(Received 21 August 2001; published 8 March 2002)

An atomic-scale description is provided for the long-range oxygen migration through the disordered SiO_2 oxide during silicon oxidation. First-principles calculations, classical molecular dynamics, and Monte Carlo simulations are used in sequence to span the relevant length and time scales. The O_2 molecule is firmly identified as the transported oxygen species and is found to percolate through interstices without exchanging oxygen atoms with the network. The interstitial network for O_2 diffusion is statistically described in terms of its potential energy landscape and connectivity. The associated activation energy is found in agreement with experimental values.

DOI: 10.1103/PhysRevLett.88.125901 PACS numbers: 66.30.–h, 61.43.Bn, 81.65.Mq

While the electronic device industry still extensively relies on silicon oxidation [1,2], the understanding of this process at the atomic scale has remained limited [3]. The widely used model proposed by Deal and Grove [4] assumes that oxygen diffuses through the oxide network before reacting at the oxide-substrate interface. Deal-Grove–like behavior was observed experimentally in thick [5] and, to some extent, also in thin oxide regimes [6,7]. However, basic issues, such as the nature of the diffusing oxygen species and the diffusion mechanism, have remained a matter of debate, both experimentally [8,9] and theoretically [10–12].

Experiments based on nuclear reaction analysis (NRA) show that the bulk of the oxide does not incorporate oxygen during oxidation, thereby favoring interstitial molecular oxygen as the migrating species [5]. This picture is also supported indirectly by the linear dependence of the diffusion on the partial pressure of the gaseous O_2 both in thermal oxides [4] and silica membranes [13], and by the similar diffusion properties of argon, an atom of approximately the same size as O_2 [14]. However, this description of the diffusion apparently contrasts with the estimate of 26 Å for the average distance between O_2 solubility sites [8], much larger than typical interatomic distances. Furthermore, very recent NRA experiments reveal the occurrence of oxygen exchange processes at the Si-SiO_2 interface, which cannot be explained by the Deal-Grove oxidation model [6] and favor atomic oxygen as the transported species [9]. Recent theoretical investigations further contribute to this intricate puzzle by suggesting diffusion mechanisms involving peroxyl [10] or ozonyl linkages [11]. However, such mechanisms would lead to oxygen exchange with the oxide network, at variance with early NRA observations [5].

We have undertaken a theoretical investigation to elucidate the long-range oxygen migration during oxidation. To account for the disordered nature of the oxide, our study evolves through three sequential steps, which progressively reduce the complexity of the theoretical framework in favor of increasing length and time scales. Using models of disordered SiO_2, we first studied within a density-functional approach the relative energetics of several oxygen species and established that interstitial O_2 is the most stable one. Then, we derived classical interatomic potentials for the O_2-network interaction from our first-principles data and extensively sampled the potential energy landscape for O_2 diffusion in a large set of disordered oxide models. Finally, we mapped the resulting energy distributions of local minima and saddle points onto a lattice model and studied the long-range diffusion properties by Monte Carlo simulations.

In our first-principles study, we used two periodic model structures of SiO_2 in which the disordered nature of the oxide is modeled by 72 independent atoms at the experimental density. In addition to a model structure, obtained previously by first-principles molecular dynamics [15], we generated a novel model structure by classical molecular dynamics [16,17]. Both structures consist of a network of cornersharing tetrahedra and show similar good agreement with diffraction data [15,18]. Structural differences are essentially limited to the ring statistics and to the distribution of interstitial volumes.

Since charged species have experimentally been ruled out as oxidizing agents in the thick oxide regime [19,20], we here focus only on neutral oxygen species. We considered atomic and molecular oxygen both as interstitial and network species. However, since the formation energy of the interstitial O_2 molecule in α quartz is found to be 3.4 eV lower than of two isolated interstitial oxygen atoms, we did not further consider the latter species in disordered SiO_2. To account for the statistical variety of sites, interstitial voids were chosen to cover the range of available cage sizes, while oxygen bridges with various Si-O-Si bond angles were selected for incorporation of network species.

To fully relax the defected structures and evaluate the associated formation energies, we used a density-functional approach [21,22]. The exchange and correlation energy was accounted for within a spin-polarized

generalized gradient approximation [23]. We used a plane-wave basis set for the electron wave functions in conjunction with norm-conserving (Si [24]) and ultrasoft (O [22]) pseudopotentials to account for the core-valence interactions. We obtained converged results with energy cutoffs of 24 and 150 Ry for the electron wave functions and augmented electron density, respectively [21,22].

We found formation energies for the network species, the peroxyl and ozonyl linkages, spread around the values calculated for α quartz (Fig. 1), without any apparent correlation with the Si-O-Si bond angle of the undefected SiO_2 structure [25]. At variance, the formation energy for interstitial molecular oxygen shows a strong correlation with the size of the interstitial void, strongly decreasing for increasing cage sizes (Fig. 1). To quantify the size of typical interstitial volumes in disordered SiO_2, we generated a large set of oxide models by classical molecular dynamics (*vide infra*). From the associated distribution of interstitial volumes (Fig. 1), we inferred that interstitial O_2 is the most stable oxygen species in the oxide. In particular, note that α quartz, used as a model in previous investigations [10,11], contains interstitials of a relatively small size giving an inappropriate description of the oxide in this respect.

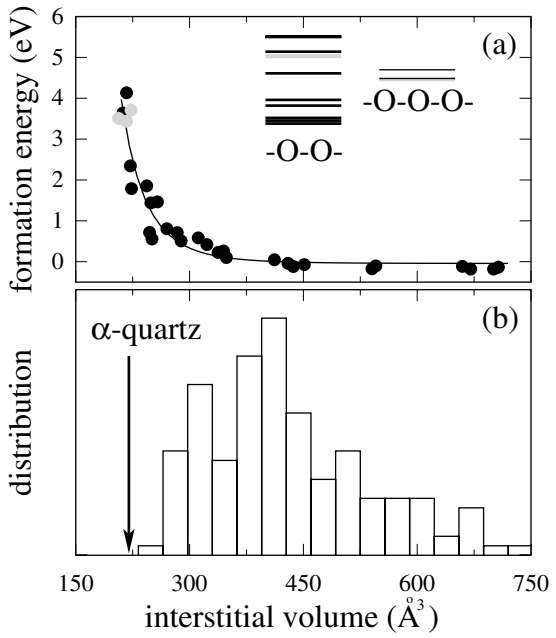

FIG. 1. (a) Formation energies for oxygen species in disordered SiO_2 (black) and α quartz (gray) calculated within a density-functional approach. The formation energies are given per pair of O atoms, with respect to the energy of the undefected SiO_2 and of the isolated O_2. The formation energies for interstitial O_2 are given vs the volume of the interstitial ellipsoid centered on the O_2 molecule. The solid line is a guide to the eye. Energy levels of the peroxyl (-O-O-) and ozonyl (-O-O-O-) linkages in α quartz and in amorphous SiO_2 are also indicated. (b) Distribution of interstitial volumes available for molecular oxygen for model structures of disordered SiO_2. The arrow indicates the value for α quartz.

To address the variety of diffusion pathways of the interstitial O_2 in a disordered network structure, it is necessary to resort to a theoretical scheme of lower computational cost. We here introduce a fully classical scheme based on interatomic pair potentials. For interactions between SiO_2 network atoms, we adopted the pair potentials of van Beest, Kramer, and van Santen [16] which well describe the vibrational excitations in vitreous silica [17]. To model the interaction between defect oxygen atoms and SiO_2 network atoms, we introduced additional Lennard-Jones–like pair potentials. The available free parameters were fixed by fitting the O_2-network interactions obtained by first principles for the local minima in Fig. 1. The resulting potentials successfully reproduced the first-principles O_2-network interactions with a rms difference of only 0.06 eV. Then, the accuracy of the classical scheme was further examined for typical diffusive motions of the O_2 molecule across barriers (*vide infra*). In particular, we selected three different barrier-crossing paths with transition energies ranging up to 2.2 eV. For discrete points along the pathway derived within our classical scheme, we fully relaxed the atomic structure by first principles, while keeping fixed the center of mass of the O_2 molecule with respect to that of the network. First-principles and classical energies always agreed within errors of less than 0.18 eV. This good agreement stems from the accurate description of the O_2-network interaction which dominates the structural relaxation.

We set out to undertake an extensive sampling of the potential energy landscape of O_2 in the oxide. By classical molecular dynamics [17], we generated a large set of model structures of disordered SiO_2, all showing the ideal connectivity. The considered set contains 19 models of different size, with a number of atoms in the periodic cell between 72 and 144. We obtained the local minima by systematic sampling of the initial O_2 positions and allowing for full structural relaxation within our classical scheme. We found a concentration of local minima of 5.4×10^{21} cm^{-3}, corresponding to an average distance between solubility sites of 5.7 Å. The considerably larger value of 26 Å estimated by Revesz and Schaeffer was obtained on the basis of the clearly inadequate assumption that all solubility sites have equal energy [8]. In fact, the energy distribution of local minima shows a finite spread (Fig. 2) as a result of the disordered nature of the oxide. Nonetheless, essentially all the energies of interstitial O_2 in local minima remain well below those of network oxygen species (Fig. 1). These results are consistent with a hopping diffusion mechanism between local minima.

To determine the connectivity between interstitials and the associated energy barriers, we searched for saddle points of the potential energy landscape defined by our classical interaction scheme. We used the activation-relaxation technique (ART) [26], which drives the system from a given local minimum to a saddle point by partially reversing the restoring force. In our case, we could apply

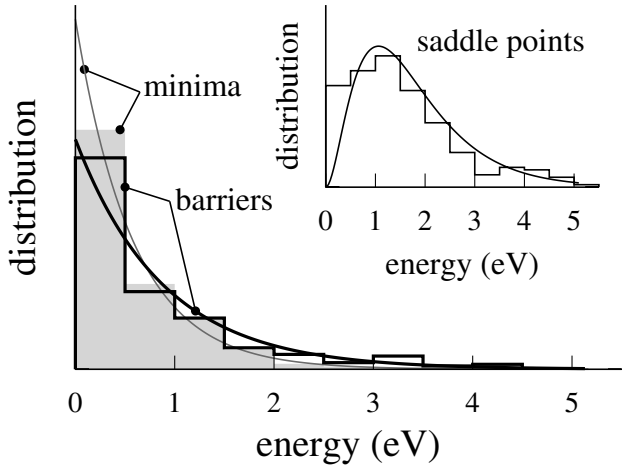

FIG. 2. Energy distributions of local minima (filled histogram) and transition barriers (open histogram) in the SiO_2 models. We here considered only the lowest transition energy for each asymmetric barrier. These distributions are well described by exponential functions (solid line) with decay constant of 0.58 and 0.88 eV, respectively. Inset: Distribution of saddle-point energies, as found for the SiO_2 models (histogram), and as obtained under the assumptions of statistical independence and of exponential functions for the distributions of local minima and transition barriers (solid line).

a simplified version of ART, in which only the force on the translational degrees of freedom of the O_2 molecule was reversed. After slightly displacing the O_2 in a random way out of a local minimum, the ART evolution was performed at a sufficiently slow rate to allow for a full relaxation of the SiO_2 network. For every local minimum, this procedure was repeated for at least 50 times, which was found to be sufficient to determine all the connections with neighboring local minima. In a few cases, to validate this approach, we also determined the saddle points using a constrained molecular dynamics technique, in which the center of mass of the O_2 molecule is dragged along the coordinate connecting neighboring minima. The saddle-point energies obtained with the two approaches coincide.

From the potential energy landscape analysis, we found all the connections between a given local minimum and its surrounding ones. The resulting random network shows an average distance between nodes of 5.3 Å and an average number of 3.3 connections per node (Table I). The calculated transition energies are described by a decaying distribution (Fig. 2), which shows a significant weight at low energies.

TABLE I. Distribution of the number of nearest-neighbor equilibrium sites obtained for the oxide models and for a cubic lattice in which connections between neighboring sites are randomly introduced according to a probability of $p = 0.55$.

	1	2	3	4	5	6
Oxide models	0.03	0.24	0.30	0.27	0.12	0.04
Lattice model	0.06	0.19	0.30	0.28	0.14	0.03

To model the long-range diffusion process in a statistically meaningful way, it is necessary to further increase the length and time scales spanned in our investigation. Therefore, we turned to a lattice model with the intent of preserving (i) the nearest-neighbor connectivity and (ii) the energy distributions of minima and saddle points, found within our classical modeling scheme. We found that a cubic lattice, in which connections between neighboring sites are introduced according to a probability of $p = 0.55$, closely reproduces the connectivity of the interstitial network in the disordered oxide models (Table I). We mapped energies onto the sites and the available connections of such a lattice model according to the extracted distributions of local minima and transition barriers. To facilitate the mapping, we described these distributions in terms of decaying exponentials (Fig. 2) and assumed *independence* between sites. Within this modeling scheme, the distribution of saddle-point energies found for the SiO_2 models is satisfactorily reproduced (Fig. 2 inset), strongly supporting the validity of the independence assumption. This also provides an *a posteriori* justification for the use of relatively small model structures to describe amorphous SiO_2.

Using Monte Carlo simulation techniques [27,28], we studied the diffusion in the lattice model for temperatures ranging between 1000 and 1500 K, which are used in the technological process of silicon oxidation. We assumed a constant attempt frequency and a unitary distance between neighboring lattice sites. The diffusion coefficient shows an effective Arrhenian temperature behavior, as frequently the case for disordered systems in specific thermal intervals [27]. The calculated activation energy of 1.12 eV, in agreement with measured values at similar temperatures (1.04–1.26 eV) [13,29,30], provides confidence in the reliability of our modeling approach. Considering only minima and saddle points actually visited in the simulation (Fig. 3), we could identify the extent of potential energies accessed by the interstitial O_2 molecule. Almost all the energies of visited minima and visited saddle points are located below the activation energy (Fig. 3). This is consistent with the percolative nature of the diffusion process, in which most of the barriers along the diffusion path are well below the activation energy. The activation energy is determined by the saddle point of highest energy which needs to be overcome to ensure long-range diffusion. These results indicate that the interstitial O_2 molecule can diffuse through the disordered network without reaching energies of competitive oxygen species (Fig. 1). In particular, this implies that the diffusion proceeds without giving rise to exchange processes with network oxygen atoms, in agreement with experimental observations [5].

To quantify the effect of the interstitial connectivity on the activation energy, we varied the probability p of

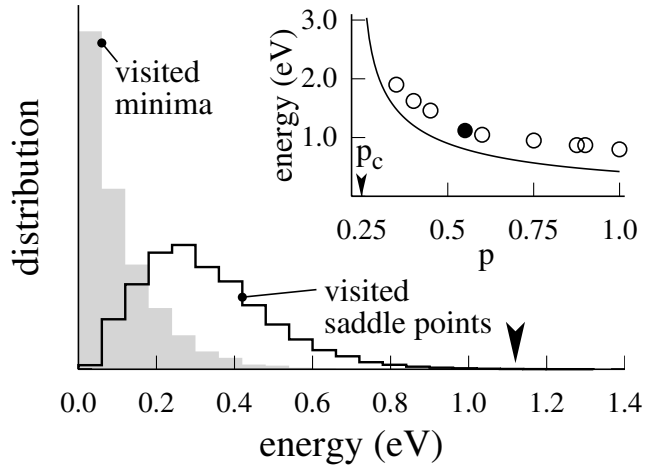

FIG. 3. Distributions of minima and saddle points visited during a Monte Carlo simulation at a temperature of 1200 K on a cubic lattice defined by $p = 0.55$. The arrow indicates the calculated activation energy for temperatures between 1000 and 1500 K. Inset: activation energy obtained by Monte Carlo simulations (dots) for the diffusion on a cubic lattice vs the probability p of introducing connections between neighboring sites. The black dot corresponds to the connectivity in disordered SiO_2 ($p = 0.55$). For comparison, we also consider a model in which all the equilibrium sites are at the same energy (solid line), and for which the activation energy can be derived from the distribution of transition energies using the percolation threshold for a cubic lattice ($p_c = 0.248\,812$) [28].

introducing connections in the lattice model, while keeping energy distributions unchanged. For increasing p, the activation energy drops monotonically until a value of 0.8 eV at $p = 1$ (Fig. 3 inset). This behavior can be naturally rationalized in terms of the amount of available diffusion pathways. Another element affecting the activation energy is the finite spread of equilibrium energies. Neglecting the asymmetry of the barriers results in a model for which the activation energy can directly be derived from the distribution of transition energies [28]. In particular, we found activation energies of 0.8 and 0.4 eV for $p = 0.55$ and 1, respectively (Fig. 3 inset). Overall, these results indicate that the activation energy for O_2 diffusion in disordered SiO_2 originates from a nontrivial interplay of both energetic and topological aspects.

The present work clearly identifies the interstitial O_2 molecule as the transported species during silicon oxidation and provides an atomistic picture of the oxygen diffusion mechanism. This study highlights the percolative nature of the diffusion process and the critical dependence of the diffusion rate on the connectivity of the interstitial network. Permeation experiments [13] on densified vitreous SiO_2 might offer an interesting case to study this relation further.

We acknowledge support from the Swiss National Science Foundation (Grants No. 21-55450.98 and No. 620-57850.99) and the Swiss Center for Scientific Computing.

[1] *Fundamental Aspects of Silicon Oxidation,* edited by Y. J. Chabal (Springer, Berlin, 2001).
[2] D. A. Muller *et al.,* Nature (London) **399**, 758 (1999).
[3] A. Pasquarello, M. S. Hybertsen, and R. Car, Nature (London) **396**, 58 (1998).
[4] B. E. Deal and A. S. Grove, J. Appl. Phys. **36**, 3770 (1965).
[5] E. Rosencher, A. Straboni, S. Rigo, and G. Amsel, Appl. Phys. Lett. **34**, 254 (1979).
[6] I. Trimaille and S. Rigo, Appl. Surf. Sci. **39**, 65 (1989).
[7] E. P. Gusev, H. C. Lu, T. Gustafsson, and E. Garfunkel, Phys. Rev. B **52**, 1759 (1995).
[8] A. G. Revesz and H. A. Schaeffer, J. Electrochem. Soc. **129**, 357 (1982).
[9] T. Åkermark, J. Electrochem. Soc. **147**, 1882 (2000).
[10] D. R. Hamann, Phys. Rev. Lett. **81**, 3447 (1998).
[11] J. R. Chelikowsky, D. J. Chadi, and N. Binggeli, Phys. Rev. B **62**, R2251 (2000).
[12] A. M. Stoneham, M. A. Szymanski, and A. L. Shluger, Phys. Rev. B **63**, 241304 (2001).
[13] F. J. Norton, Nature (London) **191**, 701 (1961).
[14] W. G. Perkins and D. R. Begal, J. Chem. Phys. **54**, 1683 (1971).
[15] J. Sarnthein, A. Pasquarello, and R. Car, Phys. Rev. Lett. **74**, 4682 (1995); Phys. Rev. B **52**, 12 690 (1995).
[16] B. W. H. van Beest, G. J. Kramer, and R. A. van Santen, Phys. Rev. Lett. **64**, 1955 (1990).
[17] K. Vollmayr, W. Kob, and K. Binder, Phys. Rev. B **54**, 15 808 (1996).
[18] S. Susman *et al.,* Phys. Rev. B **43**, 1194 (1991).
[19] D. N. Modlin and W. A. Tiller, J. Electrochem. Soc. **132**, 1659 (1985).
[20] Close to the interface, electrons might tunnel from the substrate, giving rise to negative oxygen species [12].
[21] R. Car and M. Parrinello, Phys. Rev. Lett. **55**, 2471 (1985).
[22] A. Pasquarello *et al.,* Phys. Rev. Lett. **69**, 1982 (1992); K. Laasonen *et al.,* Phys. Rev. B **47**, 10 142 (1993).
[23] J. P. Perdew and Y. Wang, Phys. Rev. B **46**, 12 947 (1992).
[24] A. Dal Corso, A. Pasquarello, A. Baldereschi, and R. Car, Phys. Rev. B **53**, 1180 (1996).
[25] M. A. Szymanski, A. L. Shluger, and A. M. Stoneham, Phys. Rev. B **63**, 224207 (2001).
[26] G. T. Barkema and N. Mousseau, Phys. Rev. Lett. **77**, 4358 (1996).
[27] Y. Limoge and J. L. Bocquet, Phys. Rev. Lett. **65**, 60 (1990).
[28] B. Roling, Phys. Rev. B **61**, 5993 (2000).
[29] E. L. Williams, J. Am. Ceram. Soc. **48**, 190 (1965).
[30] H. A. Schaeffer, J. Non-Cryst. Solids **38**, 545 (1980).